Title:

A Versatile Generator of Nanoparticle Aerosols. A novel tool in Environmental and Occupational Exposure Assessment

Authors:

Alberto Clemente[1,2], M. Pilar Lobera[1,2], Francisco Balas[1,2], Jesus Santamaria[1,2]**

[1]Instituto de Nanociencia de Aragón (INA), c/ Mariano Esquillor s/n, 50018 Zaragoza, Spain
[2]Networking Biomedical Research Centre of Bioengineering, Biomaterials and Nanomedicine (CIBER-BBN), c/ Monforte de Lemos, 28040 Madrid, Spain.

*Corresponding authors

E-mail addresses: plobera@unizar.es (M. Pilar Lobera), jesus.santamaria@unizar.es (Jesus Santamaria)

Keywords: Nanoparticle aerosol; instantaneous cloud formation; continuous aerosol stream

To cite this article: Alberto Clemente1,2, M. PilarLobera1,2*, Francisco Balas1,2, Jesus Santamaria1,2* *A Versatile Generator of Nanoparticle Aerosols. A novel tool in Environmental and Occupational Exposure Assessment,* Science of the Total Environment, 625 (2018) 978–986

DOI: 10.1016/j.scitotenv.2017.12.125

Abstract

The increasing presence of nanotechnology on the market entails a growing probability of finding ENMs in the environment. Nanoparticles aerosols are a yet unknown risk for human and environmental exposure that may normally occur during any point of the nanomaterial lifecycle. There is a research gap in standardized methods to assess the exposure to airborne nanoparticles in different environments. The controllable generation of nanoparticle aerosols has long been a challenging objective for researchers and industries dealing with airborne nanoparticles. In this work, a versatile system to generate nanoparticulate aerosols has been designed. The system allows the production of both i) instantaneous nanoparticle clouds and ii) continuous nanoparticle streams with quasi-stable values of particle concentration and size distribution. This novel device uses a compressed-air pressure pulse to disperse the target material into either the testing environment (instantaneous cloud formation) or a secondary chamber, from which a continuous aerosol stream can be drawn, with a tunable nanoparticle concentration. The system is robust, highly versatile and easy to operate, enabling reproducible generation of aerosols from a variety of sources. The system has been verified with four dry nanomaterials: TiO_2, ZnO, CuO and CNT bundles.

1. Introduction

The last decade has witnessed unprecedented development of nanotechnology as a key enabling technology, pervading all areas of activity from basic science to industrial development [1,2].The number and variety of nano-enabled consumer products is rapidly rising with extraordinary growth predictions for the next years [3].

From the environmental and health perspectives, the incidence of nanoscale matter is a matter of concern [4]. It has been shown that the presence of nanoparticle aerosols could have a significant impact in the global environment [5-8], from the upper atmosphere to ground ecotoxicology. Airborne nanoscale matter has been related to several health issues [6] through inhalation of nanoparticles [7]. Especially relevant are those engineered nanoparticles that show enhanced surface chemical features with, in turn, having a toxicological impact [8]. Since the actual toxic impact of nanoparticles will continue to be a matter of debate until sound epidemiological data can be obtained [9]; the precautionary principle should be applied when dealing with nanomaterials, especially in occupational scenarios [10].

Nanoparticle aerosols, whether intended or not, are ubiquitous in the production and handling of nanomaterials. Thus, many nanomaterial handling activities in both industrial locations and research laboratories have been shown to produce unintended aerosols containing respirable nanoparticles [11-15]. On the other hand, nanoparticle aerosols are present by design in numerous manufacturing processes for nanomaterials (e.g. flame aerosol processes, laser pyrolysis, plasma-based methods or droplet-to-particle routes) [16]. Likewise, their widespread presence a better understands dynamics of aggregation and interaction of nanoparticle aerosols with environmental particles is crucial. This, along with the importance of nanoparticle aerosols, it would be highly desirable to produce aerosols with controlled characteristics from a variety of nanomaterials. The potential application scenarios are numerous. Thus, aerosol streams with representative concentrations of a potential exposure are needed to challenge protective materials (masks, gloves) and evaluate their performance [17,18]; aerosol clouds in a controlled environment [19] would be very useful in aerosol research to validate models of aerosol dynamics and study aggregation and interaction with environmental particles [20,21]; creating tunable aerosol atmospheres would be valuable in the evaluation of the toxicity of inhaled nanoparticles in animal laboratory studies, providing a realistic alternative to the forced-inhalation and instillation systems commonly used today, etc.

There is no shortage of efforts to produce controlled nanoparticle aerosols. The most widely used method involves aerosolization of nanomaterial suspensions because it can provide aerosols from a wide variety of materials, provided that they can form stable suspensions in water or in other solvents [22]. These suspensions are dispersed in droplets, usually entrained in and air stream and produce a nanoparticle aerosol as the solvent is evaporated. The main drawbacks are related to the presence of solvent molecules in the final nanoparticle stream and to nanoparticle agglomeration during the solvent drying stage [23], with the final particle size governed by the size of the liquid droplets in the aerosol and the concentration of the nanoparticles in the starting suspension [24]. Because of its intrinsic characteristics, wet methods tend to produce aerosols that: i) have a high concentration of solvent, ii) present a wide particle size distribution, iii) face strong limitations in terms of nanoparticle concentration, and iv) are sometimes difficult to reproduce because of the variability in nanoparticle aggregation [25,26]. Some alternatives have been proposed to alleviate these problems. Thus, electrospray techniques are useful to narrow the particle size distribution [27] but face the limitation of aerosol generation depending strongly on the electrical conductivity of the solvent [28], which reduces the number of nanomaterials that could be dispersed and aerosolized [29]. Again, the limitations with this method are similar as those of conventional aerosolization: a high concentration of nanoparticles in the suspension leads to aggregates as the solvent in the drop evaporates; a low concentration produces highly diluted streams.

As an alternative, the generation of particulate aerosols from dry powders is also possible. Thus, it has been successfully employed in pharmaceutical chemistry to produce short-lived, pulsed aerosols for pulmonary drug delivery [30, 31]. Also, Venturi jets have also been used to produce micron-sized suspension droplets that after diffusion drying generate aerosol streams [32]. Other aerosolization procedures using dry powder such as attrition methods [33] and magnetic stirrer setup [34] can generate different particle concentration but the aerosol stability is a main problem. Fluidized beds setups [35] are able to aerosolize primary nanoparticles for long periods but usually lead to a low particle concentration in the aerosol, and have obvious limitations in terms of the type of nanomaterials to be aerosolized. It is worth mentioning the work of Ding and Riediker [36], who proposed a system for the continuous production of nanoparticle aerosols that are relatively stable over time. The system was effective but complex, consisting of a conical-section fluidized bed aerosolization vessel working at high pressure, followed by expansion through a critical orifice into the measurement chamber.

In this work we present a simple but versatile system, able to produce either an instantaneous cloud or a continuous air stream containing an aerosol of nanoparticles using dry nanosized powders as starting material. The device uses a compressed air pulse followed by expansion in a secondary chamber to generate a long-lasting aerosol stream with tunable nanoparticle concentration and a narrow particle size distribution (Fig. 1). The versatility of the system has been proven by aerosol generation tests using 4 different nanomaterials (Fig. 2).

2. Experimental section

2.1 Description of the aerosol generator

A scheme of the aerosol generator device is presented in Fig.1a. It consists of an air conditioning section that takes in clean, dry compressed air up to 8 bars, and a nanoparticle loading section with 40-cm^3 stainless steel reservoir, where the desired nanomaterial powder (TiO_2, ZnO, CuO, or CNT bundles) is placed after drying, on top of a 50 micron mesh at the bottom of the chamber. Both sections are connected by a fast-action valve which produces the high-pressure pulse when actioned. The pulse instantaneously disperses the target nanomaterial within the chamber and creates enough pressure to produce the exit of the nanoparticle aerosol through a 1.2 mm orifice at the top of the chamber (Fig.1b). The aerosol discharge from the chamber takes 0.1 seconds when the discharge is to atmospheric pressure (cloud formation), and longer when the discharge takes place into a secondary pressurized chamber (semicontinuous aerosol stream). Additional details are given in the caption of Fig.1.

2.2 Materials

Aeroxide® TiO_2-P25 (Evonik, Germany), ZnO (Sigma-Aldrich, USA), CuO (kindly supplied by Nanologica AB) and Multi-walled carbon nanotubes (MWCNT, Colorobbia SpA, Italy) were used for aerosol generation tests. The nanomaterials were placed in the atmospheric-pressure powder container of the nanoparticle aerosol generator (see Fig.1). TiO_2-P25, ZnO and CuO were first dried in air at 60ºC, while MWCNT were used as received. TEM images of the different nanomaterials and their particle size distribution are given in Fig.2.

2.3 Nanoparticle aerosol instantaneous cloud generation

Nanoparticle aerosols were safely released into a closed dispersion and exposure chamber [18]

in a nearly particle-free environment (less than 2 #·cm^{-3}). Briefly, this is a 13-m^3 stainless-steel chamber, equipped with an air filtering unit and a water spray self-cleaning system that allow the rapid and safe removal of airborne and deposited material. A set of sampling ports allows the characterization of the inner air, while preventing either the release of the nanoparticles to the lab or the contamination of the interior with environmental aerosols.

The nanopowder container (Fig.1c) was placed in the middle of the dispersion chamber and the air reservoir was located outside the chamber for device actuation, connected through a 1.5-m long, 5-mm inner diameter flexible rubber pipe. The pressure pulse (2-8 bar) propelled the nanoparticle load (50 to 150 g) at the base of the reservoir towards the top. The aerosol exiting through the 1.2 mm diameter orifice produced large shear forces that broke large-sized agglomerates in the solid and released the nanoparticles into the dispersion chamber. Sampling was carried out through ¼" stainless-steel pipes, located in the middle of the chamber, just below the height of the aerosol source (Fig.1b).

2.4 Aerosol characterization

Aerosols generated from dried nanoparticle powders were characterized in terms of total particle number concentration and particle size distribution. Two aerosol spectrometers were used; in the range of 5 to 500 nm, a Nano-Particle Sizer (NPS500, Particle Measuring Systems) operating in CPC and SMPS mode alternatively, and an Optical Particle Counter (OPC, Model 1.108, Grimm Aerosol), able to simultaneously classify particles from 0.3 to 20 µm in 15 size channels. The suction rates of these instruments are 0.2 and 1.2 L·min^{-1} respectably. The total particle number concentration (PNC) and particle size distributions (PSD) were followed as a function of time.

In addition to direct-reading instrument measurements, nanoparticle emissions were characterized using off-line analysis techniques on nanoparticles collected in the test chambers. Scanning electron microscopy, SEM, was performed with a FEI Inspect Field Emission Gun microscope and transmission electron microscopy, TEM, in a FEI Tecnai T20 microscope using lacey copper grids as sample holder. For SEM imaging, the sampling procedure consisted in collecting an aerosol sample within the test chambers at 1.2 L·min^{-1} for 15 s through a 50-nm mesh cellulose ester filter (Millipore) placed on top of a sample holder (Sartorius 16254) connected to a vacuum line. Aerosol sampling for TEM images was performed through lacey TEM copper grids at a flow rate of 0.2 L·min^{-1}using a state-of-the-art stainless steel aerosol

mini-sampler [35]. The morphology and size distribution of all tested materials was determined from TEM images analyzed with the image software ImageJ.

3. Results and discussion

3.1 Generation of instantaneous nanoparticle aerosol clouds

Aerosols were produced under safe conditions in a specially designed closed exposure chamber. The main characteristics of this chamber have already been reported [19] and only a brief summary is given in the Experimental section. In this work, initial aerosol generation tests were carried out with a mass of 100 mg of nanoparticulate TiO_2–P25 at pressure difference (ΔP) of 8 bar and particle-free conditions in the receiving 13 m^3 chamber. Under these conditions, the nanoparticle concentration achieved a peak value about $6 \cdot 10^4 \#\cdot cm^{-3}$ during the first minutes after emission followed by a relatively fast decrease to about $4 \cdot 10^4 \#\cdot cm^{-3}$ (67% of the peak concentration) and then by a slower decrease for the next 90 min (Fig.3a). After brief initial bursts, similar patterns have been observed: decaying rates due to agglomeration and deposition [19,37].Three independent experiments showed the cloud dispersion in the test chamber to be highly reproducible. The count median diameter (CMD) of the aerosol cloud measured 15 min after the generation was about 70 nm (Fig.3b), gradually growing to about 110 nm after 90 min inside the test chamber, reflecting the particle agglomeration dynamics for this particular system. While a similar trend is expected for other materials, the specific evolution will vary as it is well known that the behavior of the nanoparticle aerosols strongly depends on its size distribution, which affects transport, diffusion and deposition through inertia and electrostatic mechanisms [38].

Several tests were conducted with different values of ΔP and of the mass of TiO_2–P25 nanoparticles loaded into the system. As could be expected the value of ΔP has a direct effect on the concentration of nanoparticles measured at a given time in the aerosol cloud. Thus, reducing the pressure to 5 bar and 2 bar, the particle concentration in the aerosol cloud underwent a clear decrease to values of about $2.5 \cdot 10^4 \#\cdot cm^{-3}$ and $1.5 \cdot 10^4 \#\cdot cm^{-3}$respectively after 90 min of analysis in the chamber (Fig.4a), down from $3.5 \cdot 10^4 \#\cdot cm^{-3}$when the pressure of the pulse was 8 bar. Similarly, peak emission concentrations were also reduced to about $4 \cdot 10^4 \#\cdot cm^{-3}$ (ΔP=5 bar) and $2 \cdot 10^4 \#\cdot cm^{-3}$ (ΔP=2 bar) from $5.7 \cdot 10^4 \#\cdot cm^{-3}$ (ΔP=8 bar) and the time at which the maximum peak concentration was observed decreased slightly. Since the total mass loading

of TiO_2 was the same in all experiments, the decrease in the amount of nanoparticles for lower pressures in the pulse could be explained as the result of an increase in the size of aggregates. Conversely, the higher mechanical energy in the pulses at higher pressure would result in a more efficient fragmentation of aggregates and therefore an increase in the nanoparticle count.

The above explanation is consistent with the particle size distributions observed, where the largest average size was obtained for the experiment with the lower value of ΔP induced the formation of larger nanoparticles (particle size determined 15 min after aerosolization): a CMD about 110 nm was measured at ΔP of2 bar (Fig.4b). On the other hand, average particle sizes were similar for of 5 and 8 bar, indicating that at ΔP=5 bar the amount of energy is already enough to break the large aggregates. This agglomerate-breaking effect can be attributed to the shear effect during the decompression, as the aerosol discharges from the high pressure chamber through the 1.2 mm diameterorifice. Similar effects of aerodynamic hear stress on the reduction of agglomerates have been reported [36,39,40].

Fig.4c,d also show that the change in the mass of solid nanoparticles placed into the reservoir had little influence in the nanoparticle concentration and size distribution obtained after generation tests. Peak nanoparticle concentrations in the test chamber were achieved after about 10 min from emission for loadings in the range of 50 to 150 mg. Similarly, the quasi-steady state total concentration was measured at about $4 \cdot 10^4 \#\cdot cm^{-3}$ (ΔP=8 bar), with only a minor enhancement in the total number concentration when a load of 150 mg was used. The nanoparticle size distributions were also similar, with values of CMD about 70 nm in all cases.

The flexibility of the aerosol generation system allowed operating with diverse nanoparticulate materials. Similar to TiO_2–P25, aerosol cloud tests were performed using nanosized ZnO and CuO, with primary particle sizes less than 20 nm in both cases (Fig.5). Results showed that aerosol clouds could be easily formed with high reproducibility; with initial particle size distributions centered around 40 and60 nm in both cases. Also similarly to TiO_2–P25, as time increased, a shift to larger particle sizes suggesting the agglomeration of nanoparticulate aerosols within the testing environment. For the large particle size fraction (from 300 nm to 20 μm) measured with OPC a significant reduction could be observed in the larger particle size after 90 min upon cloud generation Fig.S1). Less than 1% of the total released matter had a particle size larger than 1 μm.

Fig.6 shows that the morphology of the nanoparticles collected inside the 13 m^3 testing chamber was close to that of the primary nanomaterials used for aerosol production (Fig.2). In all cases, nanoparticles were found as agglomerates with sizes about 100 nm formed by small primary nanoparticles. This is not surprising since the large agglomerates that are disaggregated during the expansion are relatively few in number, and therefore unlikely to appear in a random sampling with TEM grids or nanoparticle filters. Moreover, the agglomeration state of nanoparticles was close to that found in the starting nanosized powders, showing a fractal structure of that resembles that of nanoparticles subjected to fluidization [41,42].

Finally, the system was also tested in the generation of clouds using CNT as the target aerosol material. The results obtained by measuring with the CPC are presented in Fig. S2 although in this case the accuracy of the reading is likely to suffer due to the shape of the CNTs. In this case spectrometers were only able to detect the presence CNT aerosols in small concentrations, reflecting the difficulty of de-aggregating the CNT bundles. To study the morphology of CNT aerosols, a TEM-grid capture test was performed in the testing environment. TEM analysis clearly showed the presence of CNT bundles (Fig.7) near the emission point.

3.2 Continuous generation of nanoparticulate aerosols

In order to produce a continuous nanoparticle aerosol stream a secondary expansion cavity was added to the cloud generator described in the previous section. This 0.08-m^3stainless steel compartment was pressurized over 4 bar using dried and HEPA-filtered air and the nanoparticulate aerosol cloud was produced using 100 mg of powderedTiO_2nanomaterial at a ΔP of 8 bar. Once the nanoparticulate aerosol was dispersed in the inner volume of the cavity, an output aerosol flow was generated by opening a valve (*V4*) located at the bottom of the generation system (Fig.8).The valve aperture had to be progressively increased to obtain a constant exit flow, to compensate for the decrease of pressure in the chamber caused by the release. Typical exit flows ranged from 120 $mL \cdot min^{-1}$, a range that allowed the discharge to take place for up to 2.5 h. The duration of the discharge could readily be increased by increasing either the volume or the initial pressure of the chamber.

Fig.8 also shows the total particle concentration along time and the particle size distribution at the beginning and end of the experiment. Since now the nanoparticles are progressively released in a continuous stream rather than in an instantaneous cloud, a smaller 0.3 m^3 polycarbonate test chamber was used for the release experiments. The air contained inside the polycarbonate chamber was dried ambient particles were removed by filtration before all generation tests, in

a similar fashion as described for the large test chamber used in the cloud aerosol generation experiments. Fig.8 shows that, under the conditions used, the device produced continuous stream of TiO_2–P25 nanoparticles for periods longer than 2 hours. The nanoparticle concentration in the test chamber quickly reached a steady state value of about $5 \cdot 10^5 \#\cdot cm^{-3}$ in a 60-s period and avoided the initial burst in nanoparticle concentration. This feature is in contrast with most conventional methods for the generation of particulate aerosols from powdered materials [33-35]. This is due to the presence of the secondary expansion volume, which acts as a buffer for the initial nanoparticle aerosol cloud that is then gently released through the needle valve (Fig.8). In terms of particle size distribution in the 5 to 500 nm range, tests carried out at the beginning (10 min) and at the end (140 min) of the experiment showed narrow and nearly coincident particle size distributions with CMD values about 40 nm. This suggested that the nanoparticle aerosol remained almost unaltered during the course of the test, and agglomeration processes were negligible, with particle sizes close to those of the starting material loaded into the powder reservoir (25-30 nm). Similar tests (not shown) were carried out with ZnO and CuO nanoparticles to also obtain highly concentrated aerosols ($5 \cdot 10^5$ and $5.2 \cdot 10^5 \#.cm^{-3}$, respectively) with narrow particle size distributions. It is worth nothing that, there was a double expansion of the aerosol stream at the output of the secondary pressured cavity. It has promoted the production of nanoparticle aerosols with a smaller particle size distribution and close to the primary particles in all cases (Fig.9).

4. Conclusions

A pressure pulse in a primary chamber connected to a millimeter-size exit orifice constitutes an effective way to generate nanoparticulate aerosol clouds. The procedure is robust and reproducible, and can be applied to a variety of nanomaterials. The particle concentration within the aerosol cloud depends mainly on the pulse pressure difference, being increasing as the pressure in the pulse increases, due to a more intense fragmentation of nanoparticle aggregates. Through the addition of a secondary expansion chamber, expansion of the initial aerosol cloud could be buffered and homogenized, allowing the production of continuous nanoparticulate aerosol streams with stable particle concentration and size distributions for periods of several hours.

Supporting data

Supplementary data associated with this article can be found, in the online version.

Acknowledgements

Funding from the European Union 7th Framework Programme under the project "NanoValid, Development of reference methods for hazard identification, risk assessment and LCA of engineered nanomaterials" (Grant Agreement #263147) is acknowledged. F.B. thanks the MINECO 'Ramón y Cajal' Programme (Contract RYC-2011-07641) for financial support. M.P.L. thanks the MINECO 'Juan de la Cierva' Programme (Contract JCI-2012-13421) for financial support.

Author acknowledged the financial support of CIBER-BBN, which is an initiative funded by the VI National R&D&i Plan 2008-2011 financed by the Instituto de Salud Carlos III with assistance from the European Regional Development Fund.

1 References

[1] Lee J., Mahendra S., and Alvarez P.J.J. 2010. Nanomaterials in the construction industry: a review of their applications and environmental health and safety considerations, ACS Nano, 4, 3580-3590.

[2] van Broekhuizen P., van Veelen W., Streekstra W.H., Schulte P. and Reijnders L. 2012. Exposure limits for nanoparticles: report of an international workshop on nano reference values, Ann. Occup. Hyg., 56, 515-524.

[3] Lux Research. 2014. State of the Market Report, Nanotechnology update: corporations up their spending as revenues for nanoenabled products increase https://portal.luxresearchinc.com/research/report_excerpt/16215

[4] Wagner S., Gondikas A., Neubauer E., Hofmann T. and von der Kammer F. 2014. Spot the difference: Engineered and natural nanoparticles in the environment - Release, behaviour, and fate. Angew. Chem. Int. Ed., 53, 12398-12419.

[5] Fadeel B., Karlsson H.L. and Bhattacharya K. 2013. Geoengineering: Perilous particles. Science, 340, 548-549.

[6] Nel A., Xia T., Mädler L. and Li N. 2006. Toxic potential of materials at the nanolevel. Science, 311, 622-627.

[7] Bakand S., Hayes A. and Dechsakulthorn F. 2012. Nanoparticles: a review of particle toxicology following inhalation exposure. Inhal. Toxicol., 24, 125-135.

[8] Behra R. and Krug H.F. 2008. Nanoecotoxicology: Nanoparticles at large, Nat. Nanotechnol., 3, 253-254.

[9] Krug H.F., 2014. Nanosafety research – Are we on the right track?. Angew. Chem. Int. Ed., 53, 12304.

[10] Ding Y., Kuhlbusch T.A.J., van Tongeren M., Sánchez A., Tuinman I., Chen R., Larraza I., Mikolajczyk U., Nickel C., Meyer J., Kaminski H., Wohlleben W., Stahlmecke B., Clavaguera S. and Riediker M. 2017. Airborne engineered nanomaterials in the workplace – A review of release and worker exposure during nanomaterial production and handling processes. J. Hazard. Mater. 322, 17-28.

[11] Balas F., Arruebo M., Urrutia J. and Santamaria J. 2010. Reported nanosafety procedures in research laboratories worldwide, Nat. Nanotechnol., 5, 93-96.

[12] Gomez V., Irusta S., Balas F., Navascues N. and Santamaria J. 2014. Unintended emission of nanoparticle aerosols during common laboratory handling operations, J. Hazard.Mater.279, 75-84.

[13] Fonseca A.S., Viana M., Querol X., Moreno N., de Francisco I., Estepa C. and de la Fuente G.F. 2015. Ultrafine and nanoparticle formation and emission mechanisms during laser processing of ceramic materials, J. Aerosol Sci., 88, 48-57.

[14] Asbach, C., Neumann, V., Mons, C., Dahmann, D., van Tongeren, M. Alexander, C., Todea, A.M. 2017. On the effect of wearing personal nanoparticle monitors on the comparability of personal exposure measurements. Environ. Sci.: Nano, 4(1), 233-243.

[15] Fonseca, A.S., Maragkidou, A., Viana, M., Querol, X., Hämeri, K., de Francisco, I., Estepa, C., Borrell, C., Lennikov, V., de la Fuente, G.F. 2015. Process-generated nanoparticles from ceramic tile sintering: Emissions, exposure and environmental release. Science of the Total Environment, 565, 922-932.

[16] Sebastian V., Arruebo M., Santamaria J. 2014. Reaction engineering strategies for the production of inorganic nanomaterials. Small, 10, 835-853.

[17] Golanski, L., Guiot, A., Tardif, F. 2010. Experimental evaluation of individual protection devices against different types of nanoaerosols: Graphite, TiO_2, and Pt. Journal of Nanoparticle Research, 12(1), 83-89.

[18] Salah M.B., Hallé S., Tuduri L. 2015. Efficiency of five chemical protective clothing materials against nano and submicron aerosols when submitted to mechanical deformations. Journal of Occupational and Environmental Hygiene, 13(6), 425-433.

[19] Clemente A., Lobera M.P., Balas F. and Santamaria J. 2014. Development of a self-cleaning dispersion and exposure chamber: Application to the monitoring of simulated accidents involving the generation of airborne nanoparticles. J. Hazard. Mater., 280, 226-234.

[20] Mugica, I., Fito, C., Domat, M., Dohányosová, P., Gutierrez-Cañas, C., López-Vidal, S. 2017. Novel techniques for detection and characterization of nanomaterials based on aerosol science supporting environmental applications. Science of the Total Environment, 609, 348-359.

[21] Todea A.M., Beckmann S., Kaminski H., Bard D., Bau S., Clavaguera S., Dahmann D., Dozol H., Dziurowitz N., Elihn K., Fierz M., Lidén G., Meyer-Plath A., Monz C., Neumann V., Pelzer J., Simonow B.K., Thali P., Tuinman I., van der Vleuten A., Vroomen H., Asbach A. 2017. Inter-comparison of personal monitors for nanoparticles exposure at workplaces and in the environment. Science of the Total Environment, 605–606, 929-945.

[22] Fissan H., Ristig S., Kaminski H., Asbach C. and Epple M. 2014. Comparison of different characterization methods for nanoparticle dispersions before and after aerosolization. Anal.Methods, 6, 7324-7334.

[23] Kubo M., Nakaoka A., Morimoto K., Shimada M., Horie M., Morimoto Y. and Sasaki T. 2014. Aerosol generation by a spray-drying technique under coulomb explosion and rapid

evaporation for the preparation of aerosol particles for inhalation tests, Aerosol Sci. Technol., 48, 698-705.

[24] Gomez V., Irusta S., Balas F. and Santamaria J. 2013. Generation of TiO_2 aerosols from liquid suspensions: Influence of colloid characteristics, Aerosol Sci. Technol., 47, 1383-1392.

[25] Biskos G., Vons V., Yurteri C.U., Schmidt-Ott A. 2008. Generation and sizing of particles for aerosol-based nanotechnology. KONA Powder and Particle Journal, 26, 13-35.

[26] Ma-Hock L., Gamer A.O., Landsiedel R., Leibold E., Frechen T., Sens B., Linsenbuehler M., van Ravenzwaay B. 2007. Generation and characterization of test atmospheres with nanomaterials, Inhalation Toxicology, 19(10), 833-848.

[27] Lenggoro I.W., Xia B., Okuyama K. and Fernandez de la Mora J. 2002. Sizing of colloidal nanoparticles by electrospray and differential mobility analyzer methods, Langmuir, 18, 4584-4591.

[28] Pongrác B., Kim H.H., Negishi N. and Machala Z. 2014. Influence of water conductivity on particular electrospray modes with dc corona discharge – optical visualization approach. Eur. Phys. J. D, 68, 224-231.

[29] Gañán-Calvo A.M., López-Herrera J.M., Rebollo-Muñoz N. and Montanero J.M. 2016. The onset of electrospray: the universal scaling laws of the first ejection, Sci. Rep.,6, 32357.

[30] Ding Y., Stahlmecke B., Sánchez Jiménez A., Tuinman I.L., Kaminski H., Kuhlbusch T.A.J., van Tongeren M., Riediker M. 2015. Dustiness and deagglomeration testing: interlaboratory comparison of systems for nanoparticle powders. Aerosol Sci. Technol., 49, 1222-1231.

[31] Zhou Q., Tang P., Leung S.S.Y., Chan J.G.Y. and Chan H.K. 2014. Emerging inhalation aerosol devices and strategies: Where are we headed?. Adv. Drug Delivery Rev., 75, 3-17.

[32] Tiwari A.J., Fields C.G. and Marr L.C.. 2013. A cost-effective method of aerosolizing dry powdered nanoparticles, Aerosol Sci. Technol.,47, 1267-1275.

[33] McMahon B.W., Perez J.P.L., Yu J., Boatz J.A. and Anderson S.L. 2014. Synthesis of nanoparticles from malleable and ductile metals using powder-free, reactant-assisted mechanical attrition. ACS Appl. Mater. Interfaces, 6, 19579-19591.

[34] Stahlmecke B., Wagener S., Asbach C., Kaminski H., Fissan H., Kuhlbusch T.A.J. 2009. Investigation of airborne nanopowder agglomerate stability in an orifice under various differential pressure conditions. J. Nanoparticle Research, 11(7), 1625–1635.

[35] Clemente A., Balas F., Lobera M.P., Irusta S. and Santamaria J. 2013. Fluidized bed generation of stable silica nanoparticle aerosols. Aerosol Sci. Technol., 47, 867-874.

[36] Ding Y. and Riediker M. 2015. A system to assess the stability of airborne nanoparticle agglomerates under aerodynamic shear. J. Aerosol Sci., 88, 98-108.

[37] Anand S., Mayya Y.S., Yu M., Seipenbusch M., Kasper G. 2012. A numerical study of coagulation of nanoparticle aerosols injected continuously into a large, well stirred chamber. J. Aerosol Sci., 52, 18-32.

[38] Hinds W.C. 1999. Aerosol technology: properties, behavior, and measurement of airborne particles: second edition. John Wiley and Sons, New York.

[39] Ihalainen M., Lind T., Arffman A., Torvelaand T., Jokiniemi J. 2014. Break-up and bounce of TiO_2 agglomerates by impaction, Aerosol Sci. Technol., 48, 31-41.

[40] Ding Y., Stahlmecke B., Kaminski H., Jiang Y., Kuhlbusch T.A.J. and Riediker M. 2016. Deagglomeration testing of airborne nanoparticle agglomerates: Stability analysis under varied aerodynamic shear and relative humidity conditions. Aerosol Sci. Technol., 50, 1253-1263.

[41] de Martin L., Fabre A. and van Ommen J.R. 2014. The fractal scaling of fluidized nanoparticle agglomerates. Chem. Eng. Sci., 112, 79-86.

[42] Fabre A., Clemente A., Balas F., Lobera M.P., Santamaria J., Kreutzera M.T. and van Ommen J.R. 2017. Entrainment of nanosized clusters from a nanopowder fluidized bed. Environ. Sci.: Nano, 4, 670-678.

Figures

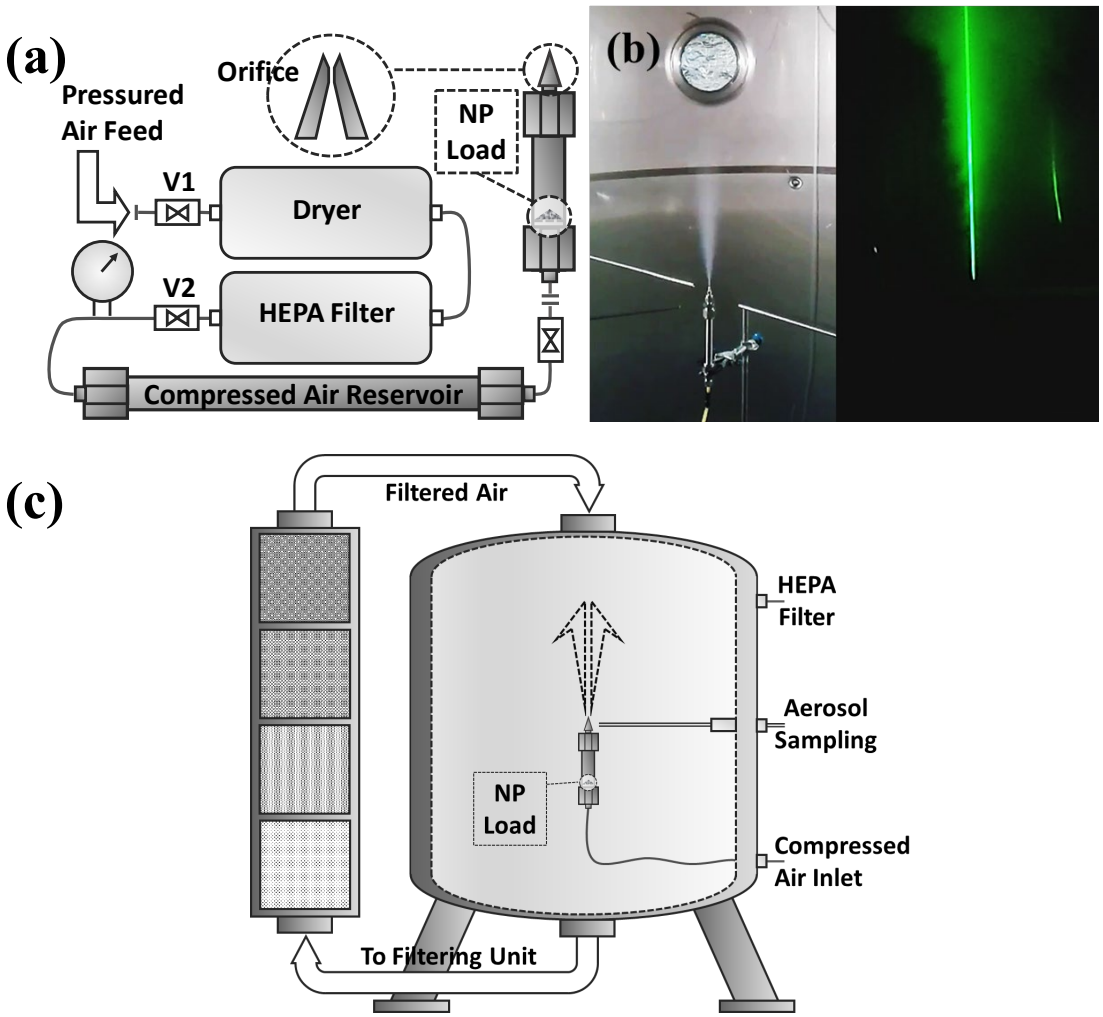

Fig.1. Description of the system for the production of nanoparticulate aerosol clouds (a) schematic of the nanoparticle aerosol generator. Dried and filtered air is compressed into a 40-cm^3 stainless steel reservoir at pressures up to 8 bar. (b) A fast action valve releases this compressed air into a second (13 cm^3) chamber that contains the dried nanosized material, dispersing it into a cloud that is expelled through a 1.2-mm orifice. (c) Scheme of aerosol cloud release into a 13 m^3 test chamber. This is a specially designed whose atmosphere can be purified to a nearly particle-free level. Real time monitoring of particle concentration was carried out by continuous sampling near the emission point and the sampled air was replaced by an equivalent volume of HEPA-filtered air.

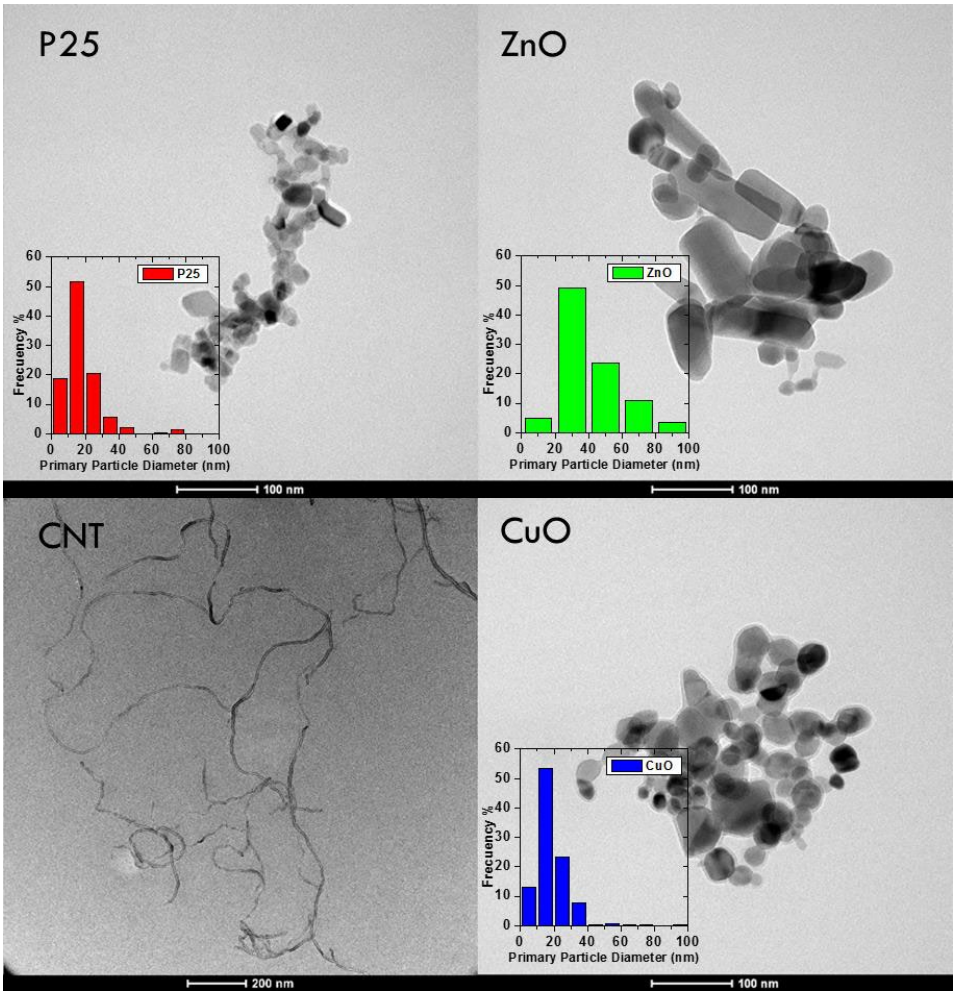

Fig.2. TEM images of the starting materials. Clockwise from the top left TiO_2–P25, ZnO, CuO and carbon nanotubes. For the powdered materials a particle size distribution is also included as inset in every figure.

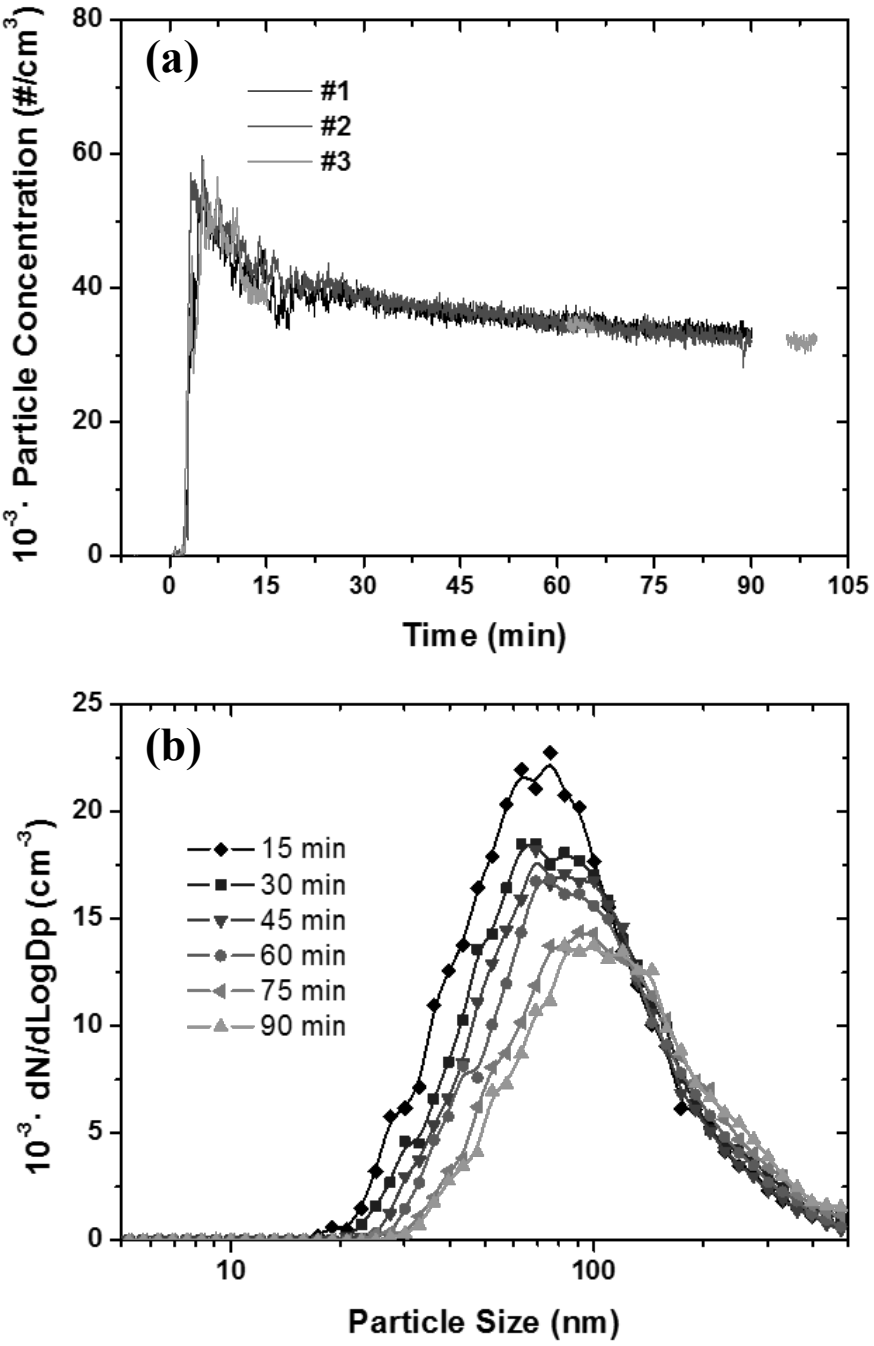

Fig.3. (a) Evolution of the total particle concentration between 5 to 500 nm following the formation of a nanoparticle cloud (100 mg of TiO_2-P25, ΔP=8 bar). The curves correspond to three independent tests. (b) Evolution of nanoparticle size distribution (5-500 nm) with time.

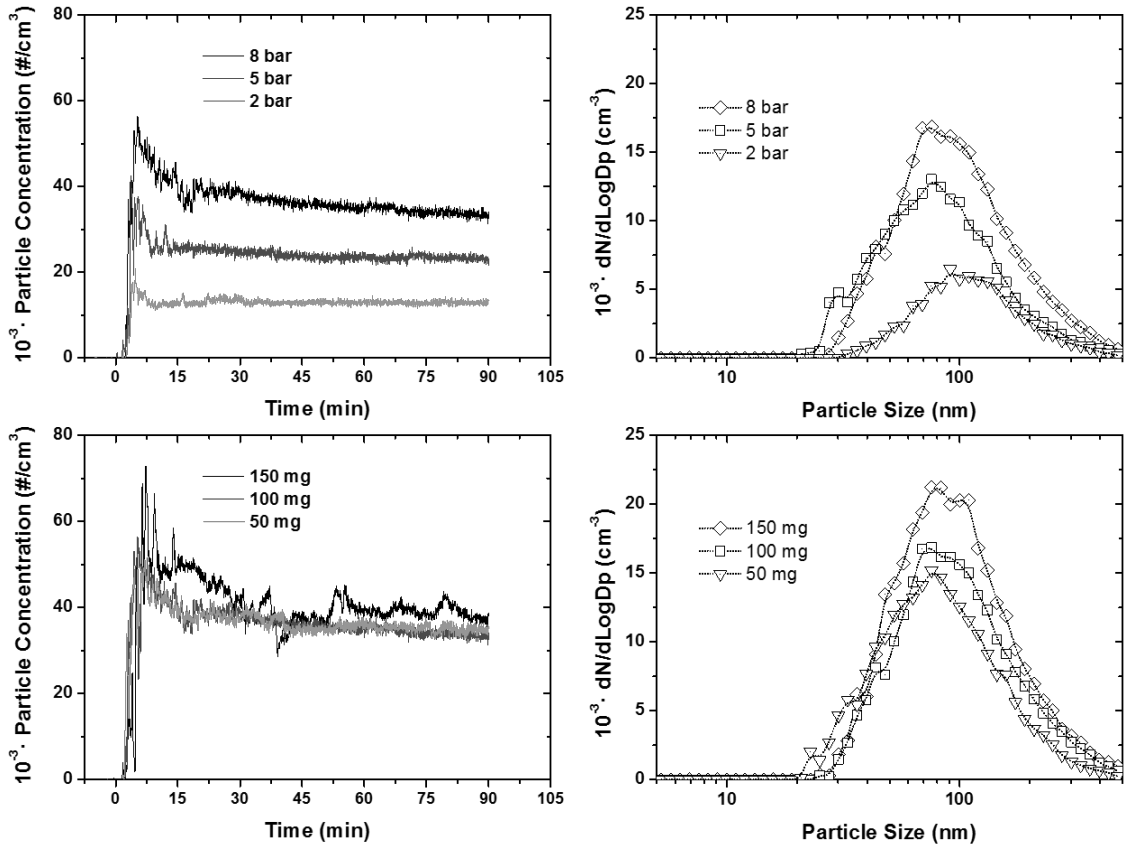

Fig.4. *Top*: Total particle concentration and particle size distribution for different values of the pressure in the dispersion pulse when dispersing a constant mass of 100 mg of TiO_2-P25 nanopowder. *Bottom*: Total particle concentration and particle size distribution for different values of the mass loaded in the chamber, for a constant pressure in the pulse of 8 bar.

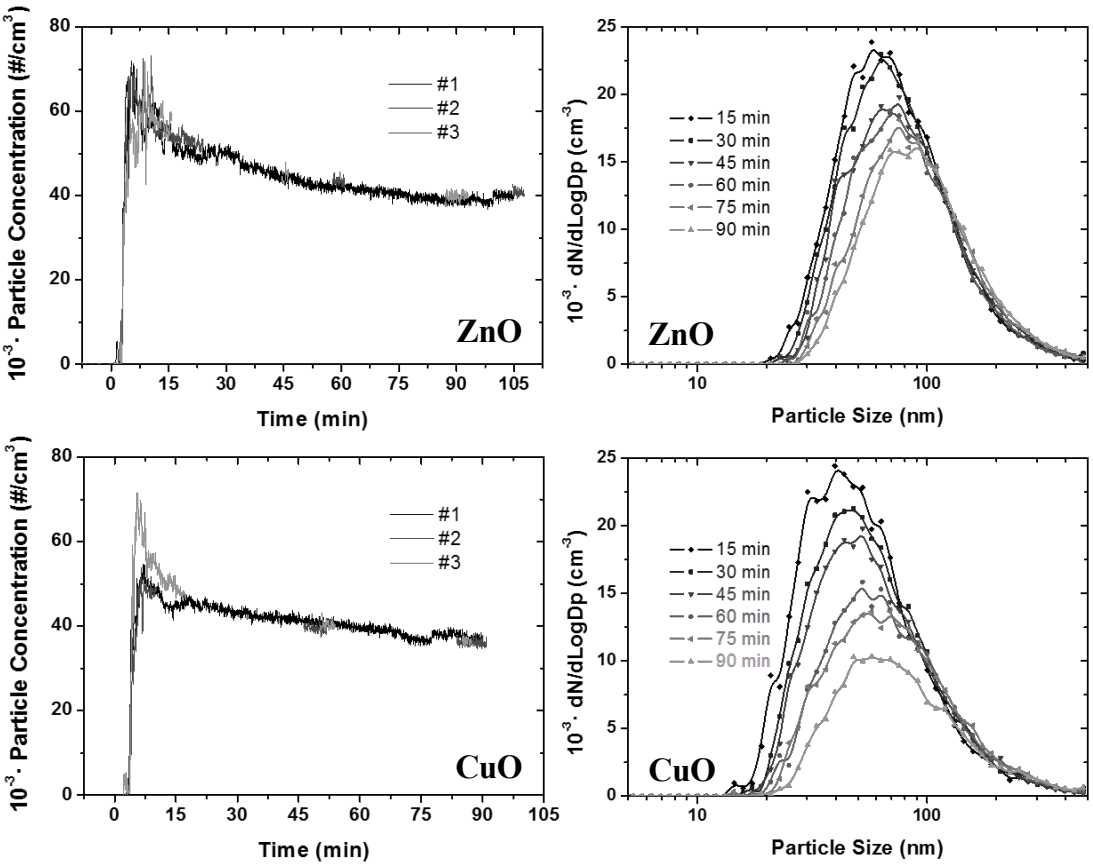

Fig.5. Total particle concentration (three independent experiments) and particle size distribution at different times when dispersing a constant mass of 100 mg of ZnO and CuO nanopowders (ΔP=8 bar).

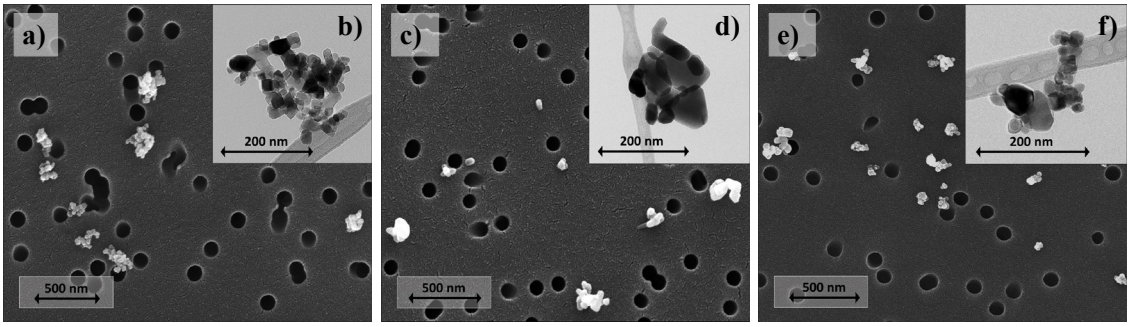

Fig.6. SEM and TEM images of the matter captured after 1 h of aerosol cloud evolution in the large (13 m^3) test chamber. (a,b) TiO_2-P25; (c,d) ZnO; (e,f) CuO.

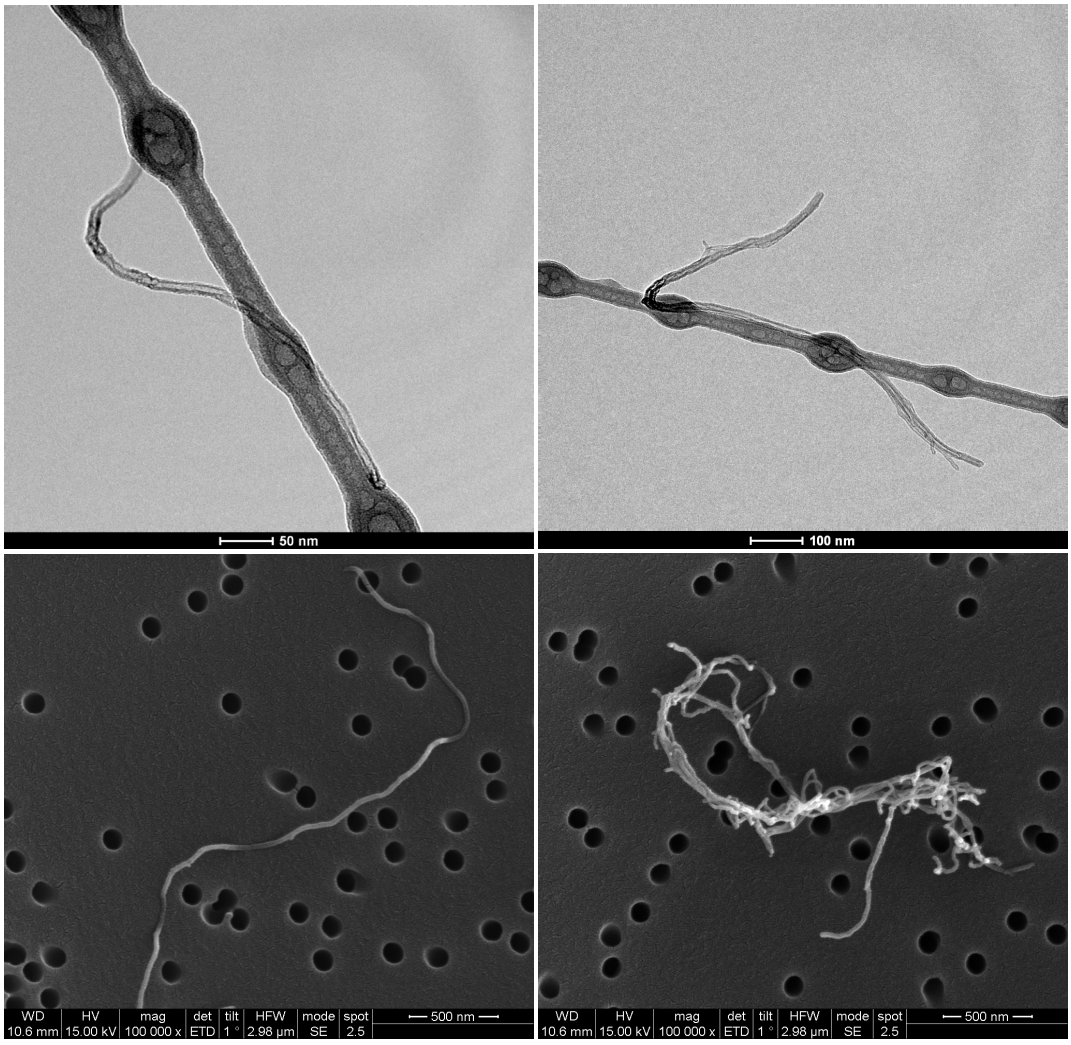

Fig.7. Particle capture tests using TEM-grid probe (*Top*) and further SEM analysis (*Bottom*) showed the presence of CNT in the testing area after cloud generation experiments with CNT (ΔP=8 bar, 100 mg) in a nearly particle-free environment (see Experimental section for details).

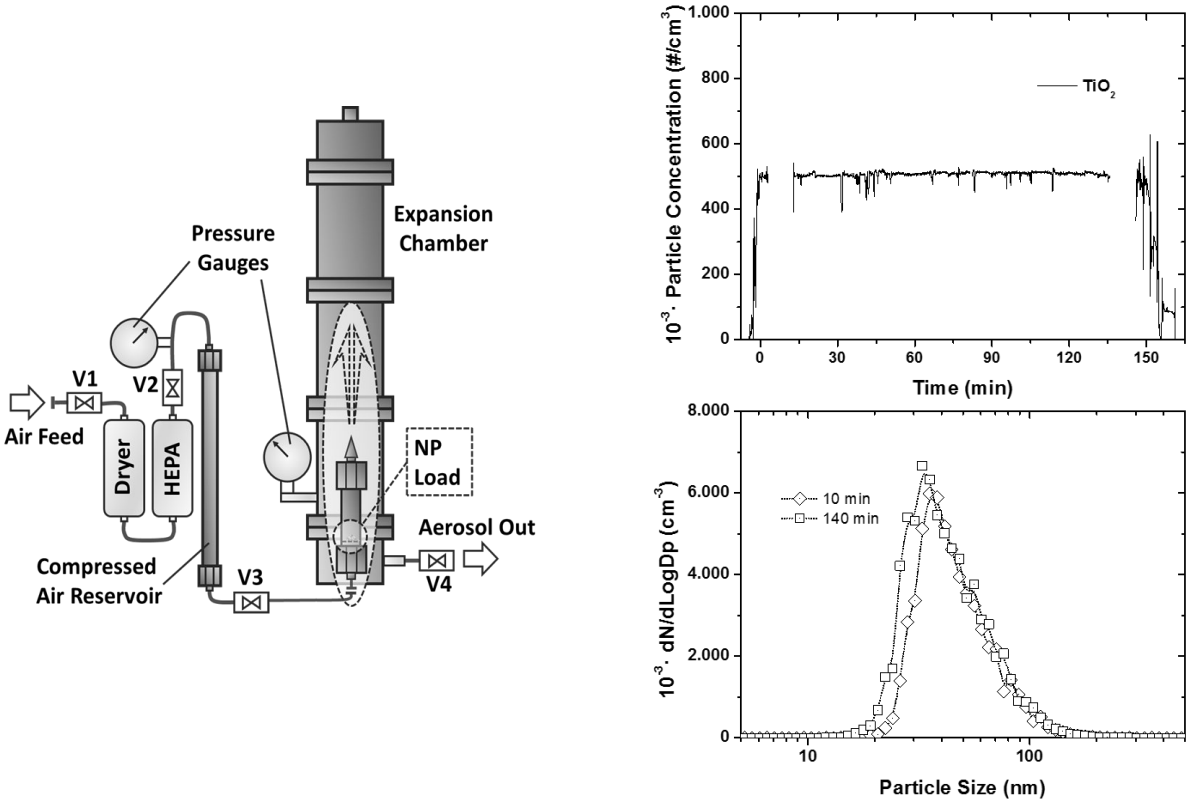

Fig.8. Description of the system for the production of continuous nanoparticulate aerosols. *Left*: Scheme showing the expansion chamber added to the cloud generation system to produce a continuous aerosol stream of nanoparticles. *Right*: (a) Total particle concentration in tests performed using TiO_2-P25 nanopowder (ΔP=8 bar, 100 mg). (b). Particle size distributions at the beginning (t=10 min) and at the end (t=140 min) of the aerosol generation tests.

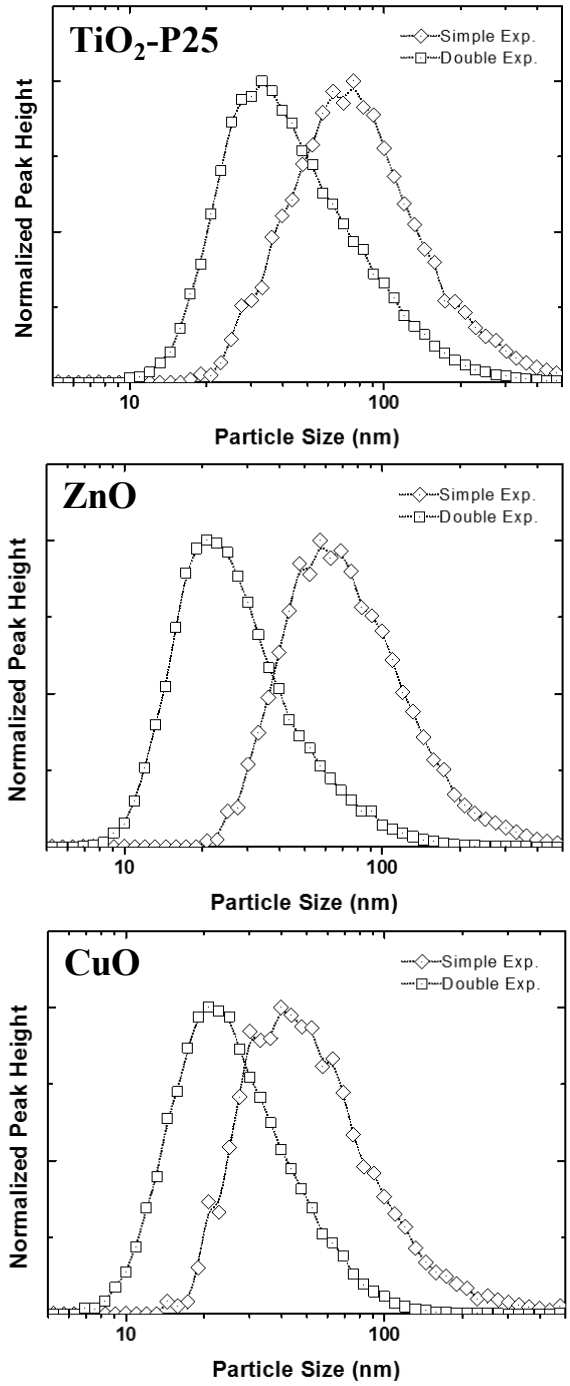

Figure 9. Comparison of particle size distribution at the beginning (t=10 min) of the aerosol generation tests (ΔP=8 bar, 100 mg) between the system for the production of instantaneous cloud of nanoparticle aerosol (simple expansion) and of continuous nanoparticulate aerosols (double expansion).